# Supplementary Material
# `AnyStar`: Domain randomized universal star-convex 3D instance segmentation

Neel Dey[1] S. Mazdak Abulnaga[1] Benjamin Billot[1] Esra Abaci Turk[2]
P. Ellen Grant[2] Adrian V. Dalca[1,3] Polina Golland[1]

[1]MIT CSAIL [2]Boston Children's Hospital, Harvard Medical School [3]Martinos Center, Massachusetts General Hospital

## A. Supplementary results

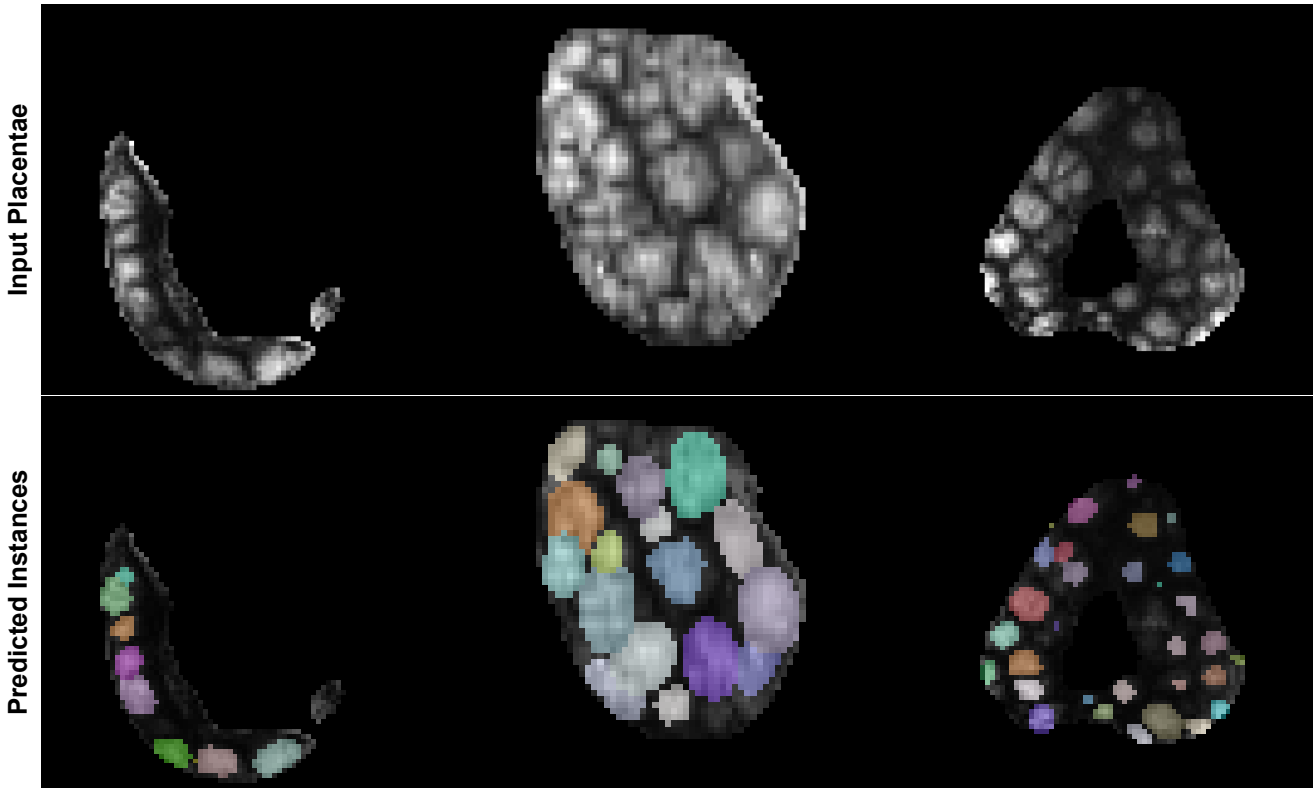


Figure 1. Qualitative 3D human placental cotyledon segmentations produced by `AnyStar-Mix`. Top: input image slices of 3D volumes, bottom: predicted objects. As ground-truth annotations are not available, we tune NMS and probability thresholds manually for qualitative visualization.

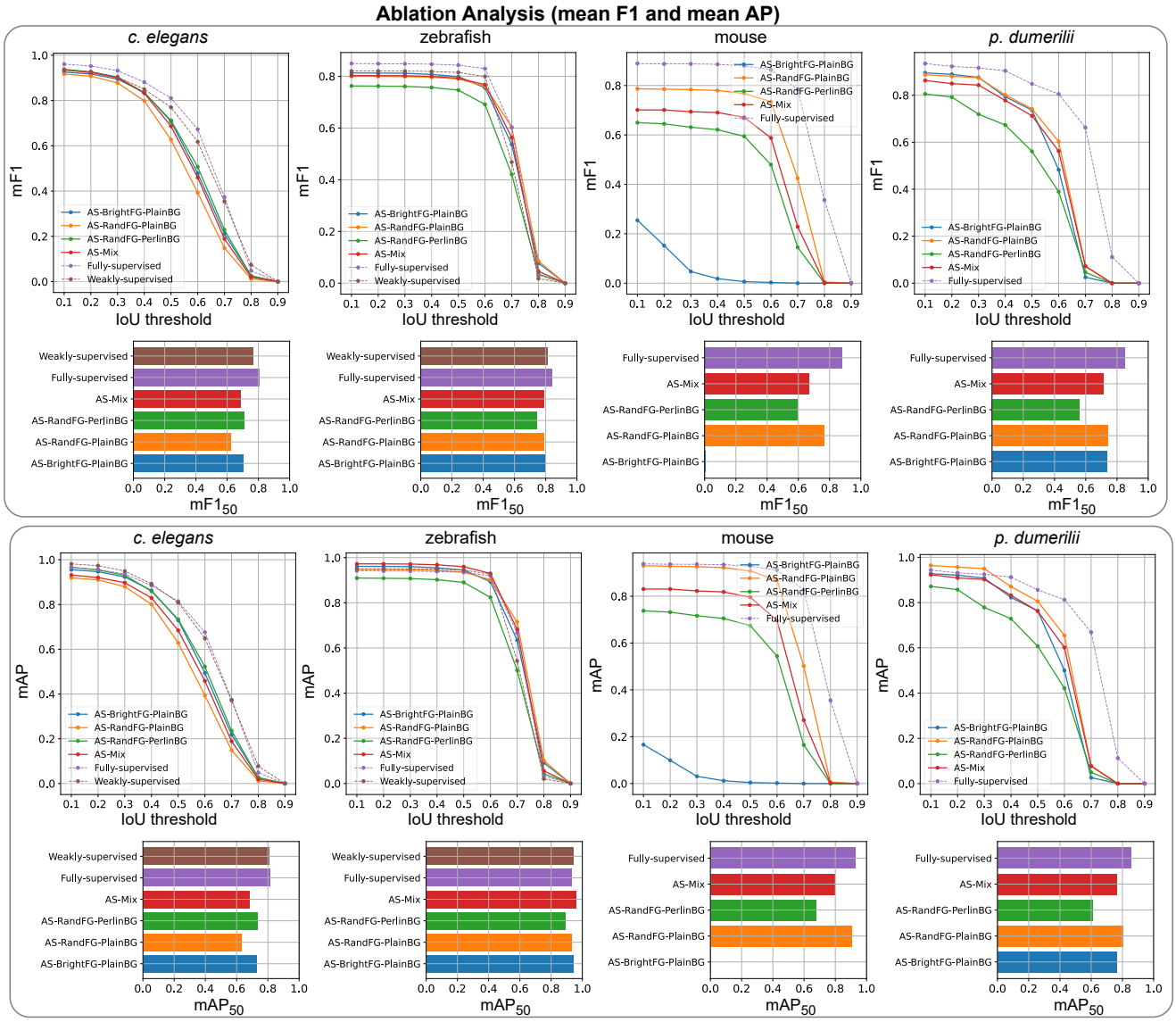


Figure 2. A companion figure to Figure 4 of the main text reporting both mean F1 (**top**) and mean average precision (**bottom**) vs. all IoU thresholds for our quantitative experiments, included for completeness.

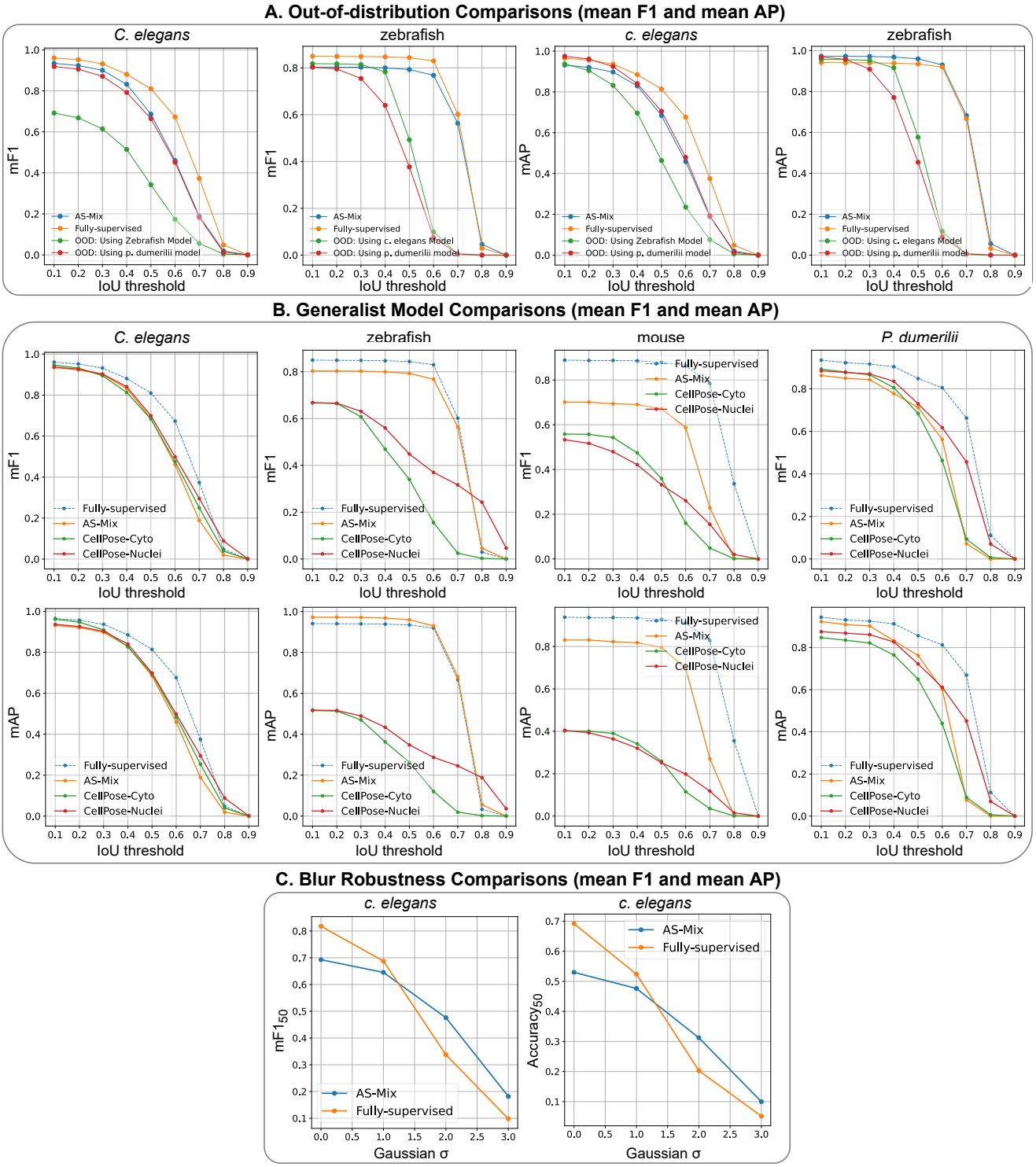


Figure 3. A companion figure to Figure 4 of the main text reporting both mean F1 and mean average precision vs. all IoU thresholds for our out-of-distribution (**A**), generalist model (**B**), and blur robustness (**bottom**) experiments, included for completeness.

## B. Additional experimental details

### B.1. Data preparation

**Placenta.** Given a fetal BOLD MRI time-series from a subject, we first exclude non-placental tissue from analysis using a publicly-available segmentation network [1]. We then motion-stabilize the temporal MRI sequence using the `ANTs` framework [10] by jointly constructing an unbiased 3D template [2, 3] and nonrigidly and diffeomorphically registering all temporal images to the template. Briefly, we use the local windowed NCC objective with a window size of 3 voxels, multi-scale registration, and B-Spline regularized SyN [9] as a deformation model. Once stabilized, intensities can be sampled within placental subregions like cotyledons and are visualized in the main paper. As only qualitative segmentations are visualized and no supervised networks are trained, no data splitting is performed.

**C. elegans.** The $yz$ plane images from [6] are cropped to a central $80 \times 80$ field-of-view and are resized to $64 \times 64$ along that plane for consistent processing across all methods. We use the dataset provided splits.

**NucMM-Z & M.** These datasets are available from [5]. As `NucMM-Z` is already provided as annotated $64 \times 64 \times 64$ crops, we do not preprocess it in any way. `NucMM-M` is downsampled by a factor of 0.6 along all axes. As test sets for the two datasets are not publicly available, we use the provided original validation sets as test sets held-out for final evaluation. `NucMM-Z`'s original training set of 27 images is further split into a new 25/2 training/validation split used for early stopping. As `NucMM-M` only has four training samples, we only use the training set for all model development and prototyping prior to final evaluation.

**PlatyISH.** Lastly, due to the high (isotropic) resolution and low SNR of `PlatyISH` [4] samples, we foreground crop and downsample by a factor of $0.4$ along all axes as this was found to benefit methods using sliding window inference (`StarDist` networks and `CellPose` [7, 8]) and to provide adequate denoising. We use the dataset provided splits. As `PlatyISH` only has two training samples, we only use the training set for all model development and prototyping prior to final evaluation.

### B.2. Other details

**Baseline augmentations.** Different augmentation pipelines are required to train on existing real data and obtain optimal performance as opposed to our approach of domain randomization which seeks to synthesize all forms of imaging artifacts and appearances from label maps. For example, real microscopy images do not typically have the MRI artifacts of bias fields, k-space spikes, Gibbs ringing, and cutout (MRI analysis often does organ-based masking). To that end, for fully and weakly supervised baselines trained on real microscopy images, we remove these MRI-specific transformations from their augmentation sequence. We retain randomized foreground cropping, gamma adjustments, blurring, histogram shifting, axis flips, 90-degree rotations, multi-distribution noise injection, and affine & elastic deformations as real microscopy image augmentations.

## References


[1] S Mazdak Abulnaga, Sean I Young, Katherine Hobgood, Eileen Pan, Clinton J Wang, P Ellen Grant, Esra Abaci Turk, and Polina Golland. Automatic segmentation of the placenta in bold mri time series. In *Perinatal, Preterm and Paediatric Image Analysis: 7th International Workshop, PIPPI*, 2022. 4

[2] Brian B Avants, Paul Yushkevich, John Pluta, David Minkoff, Marc Korczykowski, John Detre, and James C Gee. The optimal template effect in hippocampus studies of diseased populations. *Neuroimage*, 49(3):2457–2466, 2010. 4

[3] Sarang Joshi, Brad Davis, Matthieu Jomier, and Guido Gerig. Unbiased diffeomorphic atlas construction for computational anatomy. *NeuroImage*, 23:S151–S160, 2004. 4

[4] Manan Lalit, Pavel Tomancak, and Florian Jug. Embedseg: Embedding-based instance segmentation for biomedical microscopy data. *Medical Image Analysis*, 81:102523, 2022. 4

[5] Zudi Lin, Donglai Wei, Mariela D Petkova, Yuelong Wu, et al. Nucmm dataset: 3d neuronal nuclei instance segmentation at sub-cubic millimeter scale. In *Medical Image Computing and Computer Assisted Intervention–MICCAI 2021*, pages 164–174. Springer, 2021. 4

[6] Fuhui Long, Hanchuan Peng, Xiao Liu, Stuart K Kim, Eugene Myers, Dagmar Kainmüller, and Martin Weigert. 3D nuclei instance segmentation dataset of fluorescence microscopy volumes of C. elegans. *Zenodo*, Feb. 2022. 4

[7] Marius Pachitariu and Carsen Stringer. Cellpose 2.0: how to train your own model. *Nature Methods*, pages 1–8, 2022. 4

[8] Carsen Stringer, Tim Wang, Michalis Michaelos, and Marius Pachitariu. Cellpose: a generalist algorithm for cellular segmentation. *Nature methods*, 18(1):100–106, 2021. 4

[9] Nicholas J Tustison and Brian B Avants. Explicit b-spline regularization in diffeomorphic image registration. *Frontiers in neuroinformatics*, 7:39, 2013. 4

[10] Nicholas J Tustison, Philip A Cook, Andrew J Holbrook, Hans J Johnson, John Muschelli, Gabriel A Devanyi, Jeffrey T Duda, Sandhitsu R Das, Nicholas C Cullen, Daniel L Gillen, et al. Antsx: A dynamic ecosystem for quantitative biological and medical imaging. *medRxiv*, 2020. 4